Topological Insights into the Nature of the Halogen−Carbon Bonds in Dimethylhalonium Ylides and Their Cations

Alicia Jubert,*,† Nora Okulik,‡ Maria del Carmen Michelini,§ and Claudio J. A. Mota‖

CEQUINOR, Centro de Química Inorgánica (CONICET, UNLP), Departamento de Química, Facultad de Ciencias Exactas, UNLP, C. C. 962, 1900 La Plata, and Facultad de Ingeniería, UNLP, 1 y 47, 1900 La Plata, Argentina; Facultad de Agroindustrias, UNNE, Cte. Fernández 755, (3700) Pcia. R. Sáenz Peña, Chaco, Argentina; Dipartimento di Chimica and Centro di Calcolo ad Alte Prestazioni per Elaborazioni Parallele e Distribuite-Centro d'Eccellenza MURST, Università della Calabria, I-87030 Arcavacata di Rende, Italy; and Instituto de Química, Universidade Federal do Rio de Janeiro, Av Athos da Silveira Ramos 149, CT Bloco A, Cidade Universitaria, 219419-909 Rio de Janeiro, Brazil

Received: June 28, 2008; Revised Manuscript Received: September 7, 2008

In this study the nature of the bonding in a series of dimethylhalonium ylides (fluoronium, chloronium, bromonium and iodonium) was analyzed by means of topological methodologies (AIM and ELF analysis), to document the changes in the nature of the C−X bonds (X = F, Cl, Br, I) upon the series. For the sake of comparison the same study was performed on the corresponding dimethylhalonium cations ($XC_2H_6^+$) and the XCH_3 series. The wave functions used for the topological analysis were obtained at B3LYP level using extended triple-ζ basis sets. The formation of the cationic $XC_2H_6^+$ structures can be interpreted to arise from the interaction between the XCH_3 and CH_3^+ moieties. The resultant structures can be explained in terms of the superposition of two electrostatically interacting and two dative mesomeric structures. The halogen−carbon bonds have all the characteristics of the charge-shift (CS) bonds. The analysis of the C−X bond in the XC_2H_5 series shows a progressive reinforcing of the CH_3X-CH_2 bond, from FC_2H_5 that can be considered as formed from two fragments, FCH_3 and CH_2, to IC_2H_5, in which the CH_3I-CH_2 bond has all the features of a multiple bond involving atoms bearing lone pairs. Particularly interesting is BrC_2H_5, in which a special type of bond (hybrid covalent-dative double bond) has been characterized. The energetic stability of the XC_2H_5 structures with respect to the dissociation into the $XCH_2 + CH_3$ and $XCH_3 + CH_2$ ground-state fragments was studied in detail.

1. Introduction

Halonium ions[1] are very popular in organic reaction mechanisms. These stable onium ions were first proposed by Roberts and Kimball[2] to account for the stereospecificity of the addition of bromine to olefins. Olah and co-workers were the first to prepare[3] bridged-halonium ions in superacid solutions and to characterize them by spectroscopic methods. They also reported[4] that open-chain dialkylhalonium ions are formed under the same conditions. For instance, dimethylchloronium, dimethylbromonium, and dimethyliodonium were prepared by reacting the respective methyl halide with a SbF_5-SO_2 solution. The formation of the dimethylhalonium ions was characterized by deshielded singlet peaks in the NMR spectra δ at 4.1, 3.8, and 3.4, assigned to the methyl protons in the chloronium, bromonium, and iodonium ions, respectively. Dimethylbromonium and dimethyliodonium are presently commercialized as stable fluoroantimonate salts, showing their good stability at room temperature. They are good alkylating agents for aromatics, olefins, and n-donor bases.[5]

Although bridged-halonium ions have been studied thoughtfully by theoretical methods[6] the open-chain analogues have received much less attention. Olah and co-workers[7] have carried out DFT studies of the dimethylhalonium ions and found, at the B3LYP/6-31+G(d,p) level, that their structures are bent, with the C−X−C angle decreasing in the series Cl > Br > I. Charge distribution calculations have indicated that the positive charge on the halogen atom increases in the same order, as a function of the eletronegativity of the halogen atom.

SCHEME 1: Possible Resonance Structures of the Dimethylhalonium Ylides, Showing p−d δ Bonding

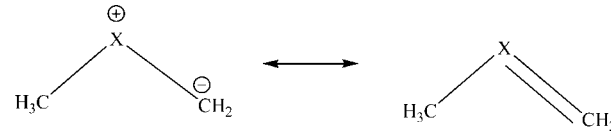

Dimethylhalonium ions are widely used in chemical ionization mass spectroscopy.[8] They are good methylating agents for a variety of compounds, such as amines, alcohols, and ethers. The reaction seems to occur through an S_N2 mechanism, with methyl halide as the leaving group but shows dependence with the thermochemistry of the formed products. For instance, the methylethylchloronium cation ($CH_3Cl^+CH_2CH_3$) reacts[8a] with amines, transferring a methyl group, whereas with ethers there is preference for transferring an ethyl group. Protonated methyl halides are also important species in chemical ionization mass spectroscopy.[9] The proton affinity of methyl halides[10] decreases with the increasing electronegativity of the halogen atom, being 155.3 kcal/mol for chloromethane, 158.1 kcal/mol for bromomethane, and 163 kcal/mol for iodomethane. On the other

* Corresponding author. E-mail: jubert@quimica.unlp.edu.ar.
† UNLP.
‡ UNNE.
§ Università della Calabria.
‖ Universidade Federal do Rio de Janeiro.

10.1021/jp805699x CCC: $40.75
Published on Web 10/16/2008

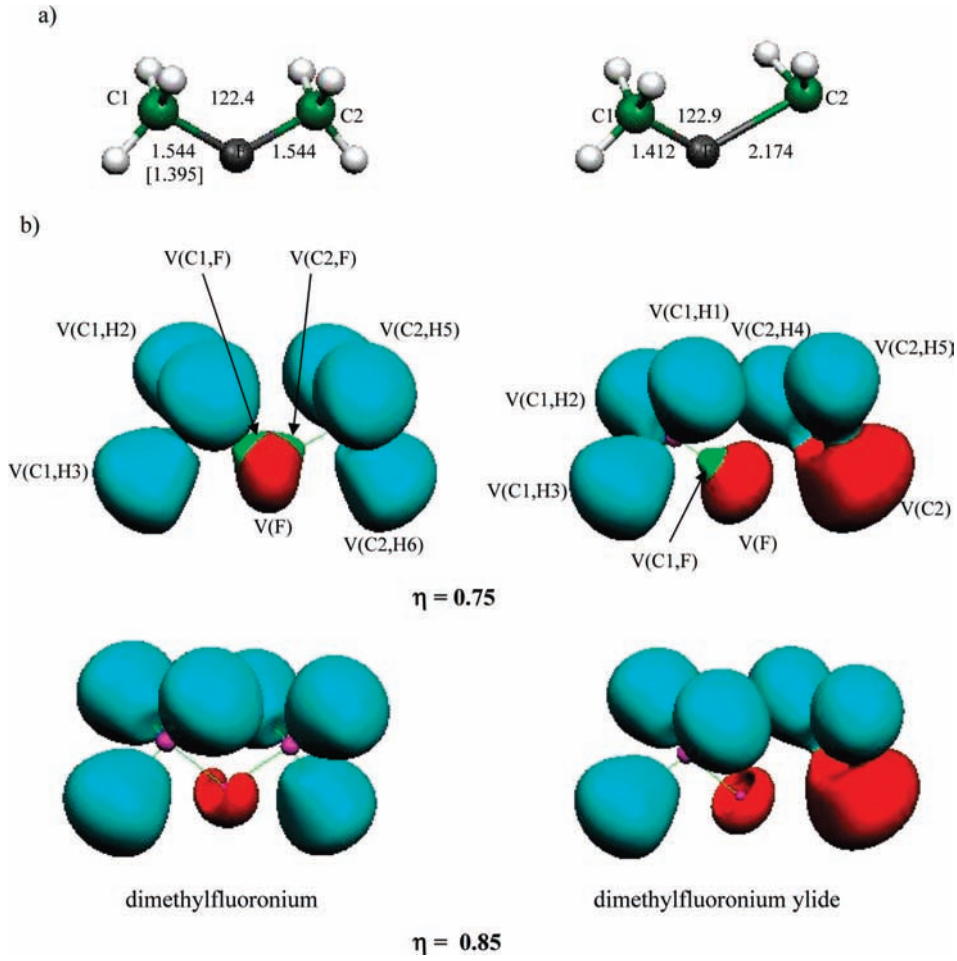

Figure 1. (a) Optimized structure of the dimethylfluoronium (left) and dimethylfluoronium ylide (right). Distances are in Å and angles in degrees. The value in square brackets corresponds to FCH_3. (b) Localization domains of the dimethylfluoronium (left) and dimethylfluoronium ylide (right).

hand, conversion of chloromethane to light olefins, such as ethene and propene, over zeolite catalysts has gained increased importance.[11] This might be an alternative process for converting natural gas into light olefins, avoiding the production of synthesis gas, as in the traditional[12] methanol to hydrocarbon process. Although the mechanism of this reaction is not completely understood, there are proposals[13] for the intermediacy of an oxonium ylide intermediate. In a similar way, there could be involvement[14] of a halonium ylide species, formed upon deprotonation of the dimethylhalonium ion on a basic site, during the catalyzed transformation of halomethanes to olefins. Because the chlorine atom has available d orbitals, there could be stabilization of the ylide through p−d π bonding (Scheme 1).

Halonium ylides have been proposed as intermediates in carbene reactions for a long time.[15] The isolation of halonium ylides was reported[16] in the reaction of diazodicyanoimidazole with aryl halides. The photochemical and metal-catalyzed reactions of R-diazoketones with alkyl and aryl halides also involves[17] the formation of halonium ylides as intermediates.

In a recent paper Noronha et al.[18] report on the gas-phase formation and structure of dimethylhalonium ylides.

The intrinsic acidity of dimethylhalonium ions has been determined, both by theoretical methods and by gas-phase reactions of the isolated ions with pyridine bases. The calculated geometry of the dimethylhalonium ions shows a bent structure with the C−X−C angle decreasing in the order Cl > Br > I. Thermochemical calculations for the reaction of the dimethylhalonium ions with pyridine, 2,6-dimethylpyridine, and 2,6-di-*tert*-butylpyridine indicate that proton transfer, with the formation of the dimethylhalonium ylide is endothermic, whereas methyl transfer, with formation of methyl halide, is exothermic. The endothermicities for proton transfer are, nevertheless, dependent on the steric hindrance of the base. The bulkier the bases, the less endothermic the proton-transfer reaction is. Experimental gas-phase reactions support the calculations, showing that methyl transfer is the major reaction of dimethylchloronium and dimethyliodonium with pyridine, whereas proton transfer, as well as single electron transfer, is observed for the bulkier bases. The calculations also indicate that acidity increases in the order chloronium > bromonium > iodonium. NBO calculations predict that hyperconjugation with the σ^* carbon-halogen orbital plays a role in stabilizing the halonium ylide species in the gas phase.

The great importance of dimethylhalonium cations and ylides as organic reaction intermediates and as methylating agents makes worth to perform a systematic analysis of the halogen−carbon bond properties, which is the key to deepen the understanding of the chemical behavior of this class of compounds. In this study the nature of the bonding in a series of dimethylhalonium ylides (fluoronium, chloronium, bromonium and iodonium) was analyzed by means of topological methodologies, to document the changes in the nature of the C−X bonds (X = F, Cl, Br, I) upon the series. With the aim of comparison, the same study was performed on the corresponding dimethylhalonium cations and the XCH_3 series. In addition, the

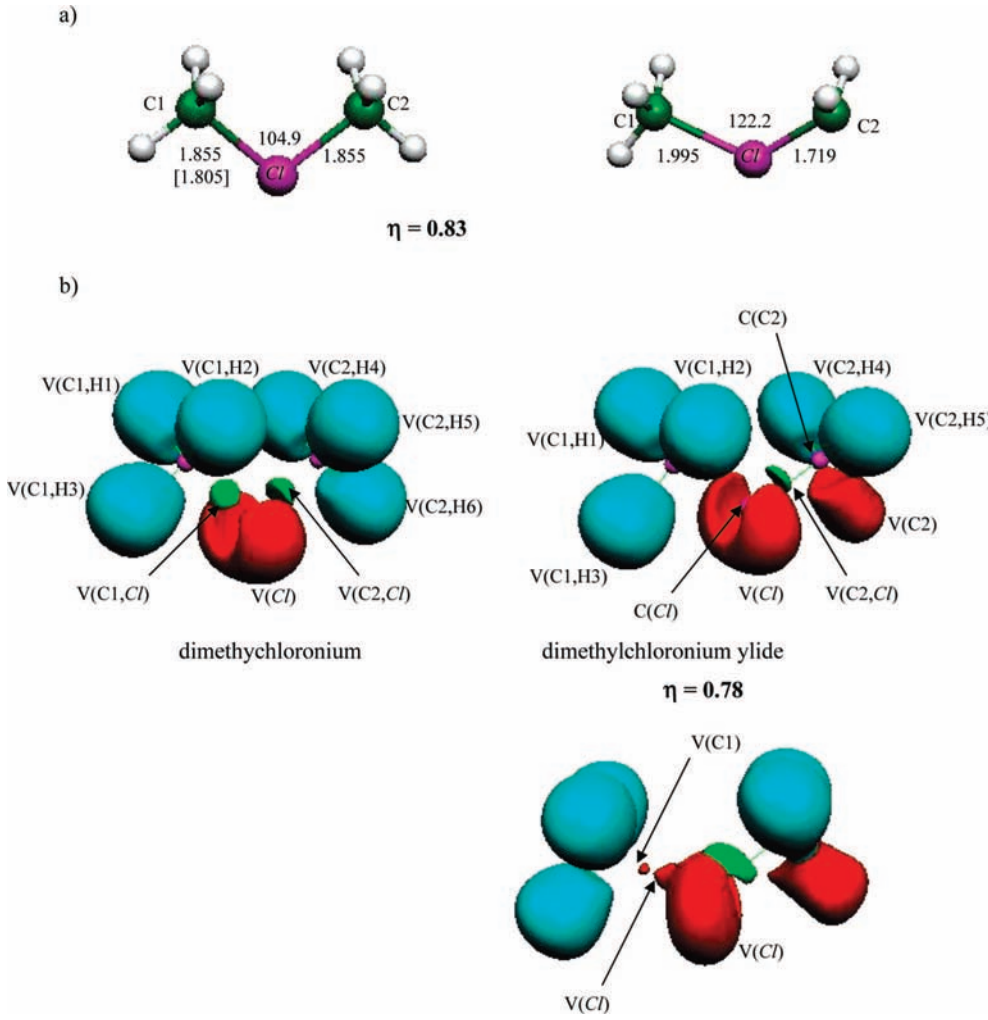

Figure 2. (a) Optimized structure of the dimethylcholorium (left) and dimethylcholorium ylide (right). Distances are in Å and angles in degrees. The value in square brackets corresponds to $ClCH_3$. (b) Localization domains of the dimethylcholorium (left) and dimethylfluoronium ylide (right).

energetic stability of the dimethylhalonium ylides with respect to the dissociation into $XCH_2 + CH_3$ and $XCH_3 + CH_2$ fragments was studied in detail.

2. Methodology

2.1. AIM Analysis. The atoms-in-molecules (AIM) theory[19] reveals insightful information on the nature of bonds. This theory is based on the critical points (CP) of the electronic density, $\rho(\mathbf{r})$. These are points where the gradient of the electronic density, $\nabla\rho(\mathbf{r})$, vanishes and are characterized by the three eigenvalues (λ_1, λ_2, λ_3) of the Hessian matrix of $\rho(\mathbf{r})$. The CPs are labeled as (r,s) according to their rank, r (number of nonzero eigenvalues), and signature, s (the algebraic sum of the signs of the eigenvalues).

Four types of CPs are of interest in molecules: (3,−3), (3,−1), (3,+1), and (3,+3). A (3,−3) point corresponds to a maximum in $\rho(\mathbf{r})$ and occurs generally at the nuclear positions. A (3,+3) point indicates electronic charge depletion and is known as cage CP. (3,+1) points, or ring CP, are merely saddle points. Finally, a (3,−1) point or bond critical point (BCP), is generally found between two neighboring nuclei indicating the existence of a bond between them. Several properties that can be evaluated at a bond critical point (BCP) constitute very powerful tools to classify the interactions between two fragments.

The two negative eigenvalues of the Hessian matrix (λ_1 and λ_2) at the BCP measure the degree of contraction of $\rho(\mathbf{r})$ perpendicular to the bond toward the critical point, whereas the positive eigenvalue (λ_3) measures the degree of contraction parallel to the bond and from the BCP toward each of the neighboring nuclei. Unequal values of λ_1 and λ_2 at (3,−1) BCP's denote an anisotropic spread of electrons quantified through the concept of ellipticity: $\varepsilon = \lambda_1/\lambda_2 - 1$, (with $\lambda_1 > \lambda_2$) where values of $\varepsilon \gg 1$ can be indicative of π bonding. Calculated properties at the BCP of the electronic density are labeled with the subscript "b" throughout the work.

In the AIM theory atomic interactions are classified according to two limiting behaviors, namely, shared interactions and closed-shell interactions. Shared interactions are characteristic of covalent and polarized bonds and their main features are large values of ρ_b, $\nabla^2\rho_b < 0$ and $E_b < 0$, E_b being the local electronic energy density of the system calculated at the BCP and defined as the sum of the local kinetic energy density and the local potential energy density, both computed at the BCP. In contrast, closed-shell interactions, useful to describe ionic bonds, hydrogen bonds, and van der Waals interactions, are characterized by small values of ρ_b, $\nabla^2\rho_b > 0$ and $E_b > 0$. Within the framework of AIM analysis the variance, $\sigma^2(\Omega_A)$, of the atomic basin populations can be spread in terms of the contribution from other basins, the covariance, $\mathrm{cov}(\Omega_A, \Omega_B)$, which has a clear relationship with the so-called delocalization index, $\delta(\Omega_A, \Omega_B)$[20a,b]

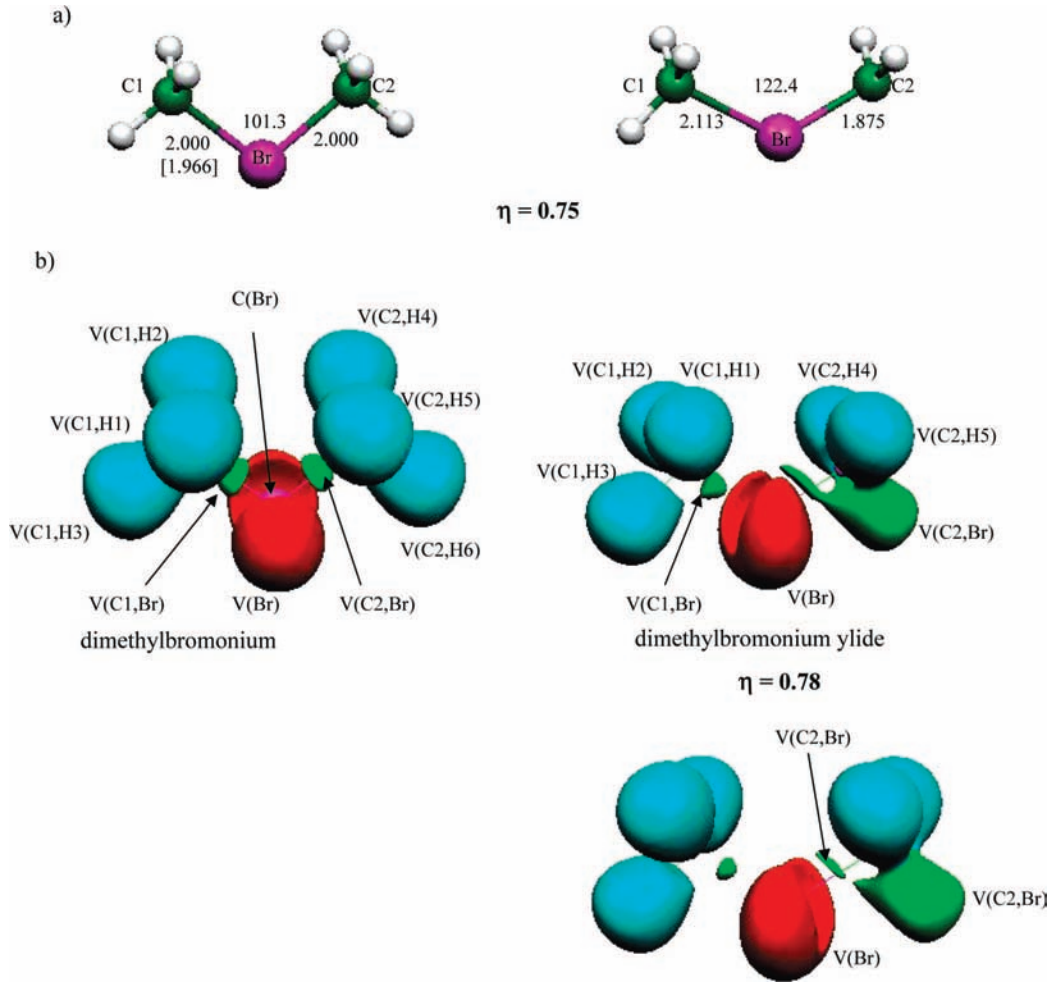

Figure 3. (a) Optimized structure of the dimethylbromonium (left) and dimethylbromonium ylide (right). Distances are in Å and angles in degrees. The value in square brackets corresponds to $BrCH_3$. (b) Localization domains of the dimethylbromonium (left) and dimethylbromonium ylide (right).

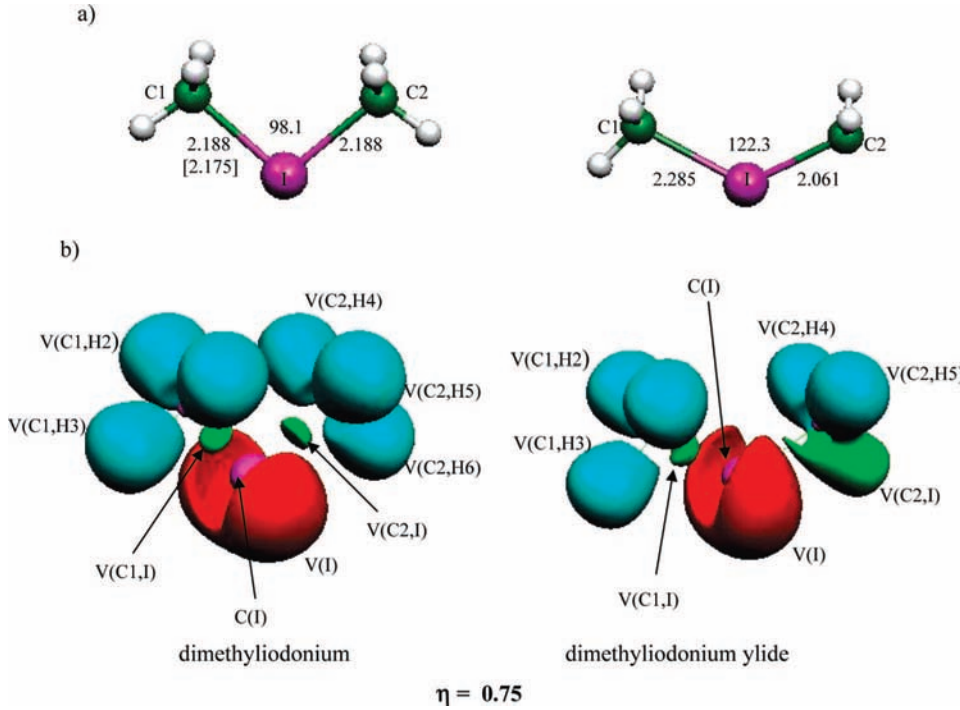

Figure 4. (a) Optimized structure of the dimethyliodonium (left) and dimethyliodonium ylide (right). Distances are in Å and angles in degrees. The value in square brackets corresponds to ICH_3. (b) Localization domains of the dimethyliodonium (left) and dimethyliodonium ylide (right).

$$\mathrm{cov}(\Omega_A,\Omega_B) = -\delta(\Omega_A,\Omega_B)/2$$

The delocalization index accounts for the electrons delocalized or shared between the basins Ω_A and Ω_B. In the single determinant approach this index is exactly the topological bond order defined by Ángayán and co-workers.[20c] We must mention, however, that even when for molecular bonds with equally shared pairs a simple relationship between the delocalization index and the formal bond order (number of Lewis bonded pairs) has been generally found,[20d] for polar bonds there is no longer such a simple relationship. It has been shown that the delocalization index tend to decrease with the increased electronegativity difference of the atoms involved in the bond. There has been some discussion in the past regarding the use of this index as a covalent bond order.[20d,e]

2.2. ELF Analysis. The electron localization function (ELF) analysis is based on the topology of the gradient vector field of the Becke and Edgecombe[21] electron localization function, as implemented by Silvi and Savin.[22] The ELF has been suggested to be a measure of the excess of kinetic energy density due to the Pauli repulsion[23]

$$\eta(r) = \frac{1}{1+\left(\frac{D_\sigma(r)}{D_\sigma^0(r)}\right)}$$

where $D_\sigma(r)$ is the local excess kinetic energy density due to Pauli repulsion and $D_\sigma^0(r)$ is the kinetic energy density of a reference homogeneous electron gas of the same electron density, a value that essentially acts as a renormalization factor.

Values of $\eta(r)$ thus range from 0 to 1 with larger values denoting larger electron localization, i.e., a higher probability of finding electrons alone or in pairs of antiparallel spin. The gradient field of the ELF, $\nabla\eta(r)$, can be also used to partition the space into localization basins, Ω_A.[22] Each of these basins contains a (3,−3) critical point of $\eta(r)$, also referred to as an attractor, which may or may not contain an atomic center. Basins are visualized for any given isodensity value of $\eta(r) = f$, which in turn encompass regions of $\eta(r) \geq f \leq 1$. Basins are classified as either (1) core basins, C(A), encompassing a nucleus ($Z > 2$) and core electrons, or as (2) valence basins, V(A,...), encompassing valence shell electrons.[22] Valence basins are furthermore categorized by their synaptic order, which refers to the number of core basins with which they share a common boundary. A monosynaptic basin, V(A), encompasses lone pairs whereas a polysynaptic basin, V(A,...), encompasses electrons involved in bi- or polycentric bonds. The presence of a di- or polysynaptic basin is indicative of a shared interaction of electrons (covalent, dative, or metallic bonds), whereas its absence denotes a closed-shell interaction (ionic, van der Waals or hydrogen bond). Basin-related properties are calculated by integrating a certain property over the volume of the basin. For instance, the electronic population of a synaptic basin, $\bar{N}(\Omega_A)$, is obtained as the integral of the one-electron density over the basin Ω_A. The variance of the basin population, $\sigma^2[\bar{N}(\Omega_A)]$, which is the square of the standard deviation of the population, represents the quantum-mechanical uncertainty of the basin population and is a consequence of the delocalization of electrons. It has the meaning of an excess in the number of pairs due to the interaction of Ω_A with other basins and is usually written as the sum of contributions of all other basins. Within ELF analysis a multiple bond is characterized by a basin population $\bar{N}(\Omega_A)$ higher that 2.0 electrons and a variance $\sigma^2[\bar{N}(\Omega_A)]$ lesser than the corresponding basin population. The topological representation obtained from ELF analysis, is usually interpreted in terms of superposition of mesomeric structures.[24]

3. Computational Details

Molecular geometries were optimized within the density functional theory (DFT) approach at the B3LYP/6-311++G(d,p) level.[25,26] For iodine we have used the 6-311G(d)[26] basis set,

TABLE 1: Topological Properties of Charge Density[a,b] Calculated at C−X BCP's of Dimethylhalonium and Dimethylhalonium Ylide[c]

	dimethylfluoronium				dimethylfluoronium ylide			
bond[d]	ρ_b	$\nabla^2\rho_b$	ε	E_b	ρ_b	$\nabla^2\rho$	ε	E_b
C1−F	0.1425 [0.2280]	0.0825 [0.0038]	0.0682 [0.0005]	−0.1342 [−0.2895]	0.2160	0.0209	0.0014	−0.2677
C2−F	0.1425	0.0825	0.0682	−0.1342	0.0334	0.1242	0.0230	−0.0008
	dimethylchloronium				dimethylchloronium ylide			
bond[d]	ρ_b	$\nabla^2\rho_b$	ε	E_b	ρ_b	$\nabla^2\rho$	ε	E_b
C1−Cl	0.1501 [0.1729]	−0.1437 [−0.2063]	0.0222 [0.0000]	−0.0923 [−0.1081]	0.1217	−0.0127	0.0603	−0.0944
C2−Cl	0.1501	−0.1437	0.0222	−0.0923	0.1902	−0.2168	0.2310	−0.1497
	dimethylbromonium				dimethylbromonium ylide			
bond[d]	ρ_b	$\nabla^2\rho_b$	ε	E_b	ρ_b	$\nabla^2\rho$	ε	E_b
C1−Br	0.1308 (0.1309) [0.1405]	−0.1017 (−0.1019) [−0.1130]	0.0370 (0.0370) [0.0000]	−0.0667 (−0.0667) [−0.0723]	0.1100 (0.1101)	−0.0240 (−0.0242)	0.0648 (0.0643)	−0.0446 (−0.0447)
C2−Br	0.1308 (0.1309)	−0.1017 (−0.1019)	0.0370 (0.0370)	−0.0667 (−0.0667)	0.1567 (0.1566)	−0.1094 (−0.1094)	0.1949 (0.1946)	−0.0947 (−0.0947)
	dimethyliodonium				dimethyliodonium ylide			
bond[d]	ρ_b	$\nabla^2\rho_b$	ε	E_b	ρ_b	$\nabla^2\rho$	ε	E_b
C1−I	(0.1089) [0.1087]	(−0.0647) [−0.0310]	(0.0618) [0.0000]	(−0.0485) [−0.0479]	(0.0929)	(−0.0107)	(0.0791)	(−0.0356)
C2−I	(0.1089)	(−0.0647)	(0.0618)	(−0.0485)	(0.1274)	(−0.0271)	(0.1759)	(−0.0658)

[a] ρ_b, $\nabla^2\rho_b$ and E_b in au. [b] Calculated at the B3LYP/6-311G++(d,p) level. Values in parentheses were obtained using the 6-311G(d) basis sets for the halogen atom. [c] With the aim of comparison the values for the XCH_3 compounds are reported in square brackets. [d] For the label of the atoms see Figures 1−4.

TABLE 2: Basin Populations ($\bar{N}$), Atomic Contributions to Each Basin, and Variance of the Basins, $\sigma^2(\bar{N})$ for Dimethylfluoronium and Dimethylfluoronium Ylide[a,b]

dimethylfluoronium				dimethylfluoronium ylide			
basin	$\bar{N}$	atomic contribution	σ^2 ($\bar{N}$)	basin	$\bar{N}$	atomic contribution	$\sigma^2(\bar{N})$
C(C1)	2.08 [2.09]	2.08 [2.09] (C1)	0.25 [0.51]	C(C1)	2.09	2.09 (C1)	0.26
C(C2)	2.08	2.08 (C2)	0.25	C(C2)	2.07	2.07 (C2)	0.23
C(F)	2.14 [2.12]	2.14 [2.12] (F)	0.39 [0.38]	C(F)	2.14	2.14 (F)	0.38
V(H1,C1)	2.02 [2.06]	1.19 [1.10] (C1) 0.82 [0.93] (H1)	0.60 [0.62]	V(H1,C1)	2.04	1.12 (C1) 0.91(H1)	0.62
V(H2,C1)	2.03 [2.05]	1.23 [1.11] (C1) 0.79 [0.93] (H2)	0.60 [0.62]	V(H2,C1)	2.05	1.13 (C1) 0.91(H2)	0.62
V(H3,C1)	2.08 [2.06]	1.25 [1.11] (C1) 0.82 [0.93] (H3)	0.61 [0.62]	V(H3,C1)	2.07	1.14 (C1) 0.91(H3)	0.63
V(H4,C2)	2.02	1.20 (C2) 0.82 (H4)	0.60	V(H4,C2)	1.96	0.97 (C2) 0.98 (H4)	0.58
V(H5,C2)	2.03	1.23 (C2) 0.79 (H5)	0.60	V(H5,C2)	1.91	0.93 (C2) 0.98 (H5)	0.57
V(H6,C2)	2.07	1.25 (C2) 0.82 (H6)	0.61				
V(F)	2.87 [2.24, 2.12][c]	2.87 [2.24,2.12] (F)	1.27 [1.09,1.07]	V(F)	3.43	3.43 (F)	1.38
V(C2,F)	0.81	0.07 (C2) 0.74 (F)	0.60				
V(F)	2.93 [2.26][c]	2.93 [2.26] (F)	1.28 [1.10]	V(F)	3.23	3.22 (F)	1.34
V(C1,F)	0.81 [0.92]	0.74 [0.76] (F) 0.07 [0.16] (C1)	0.60 [0.67]	V(C1,F)	0.88	0.15 (C1) 0.74 (F)	0.64
				V(C2)	2.12	2.10 (C2)	0.70

[a] All quantities are in electrons. [b] With the aim of comparison the values for the XCH_3 compounds are reported in square brackets. [c] There are three monosynaptic V(F) basins in FCH_3.

TABLE 3: Basin Populations ($\bar{N}$), Atomic Contributions to Each Basin, and Variance of the Basins, $\sigma^2(\bar{N})$ for Dimethylchloronium and Dimethylchloronium Ylide[a,b]

dimethychloronium				dimethylchloronium ylide			
basin	$\bar{N}$	atomic contribution	$\sigma^2(\bar{N})$	basin	$\bar{N}$	atomic contribution	$\sigma^2(\bar{N})$
C(C1)	2.09 [2.09]	2.09 [2.09] (C1)	0.26 [0.26]	C(C1)	2.09	2.08 (C1)	0.25
C(Cl)	10.04 [10.06]	10.04 [10.06] (*Cl*)	0.56 [0.56]	C(Cl)	10.07	10.06 (*Cl*)	0.56
C(C2)	2.09	2.09 (C2)	0.26	C(C2)	2.09	2.09 (C2)	0.26
V(H1,C1)	2.00 [2.04]	1.17 [1.13] (C1) 0.83 [0.91] (H1)	0.63 [0.65]	V(H1,C1)	2.10	1.20 (C1) 0.91 (H1)	0.68
V(H2,C1)	2.06 [2.04]	1.22 [1.13] (C1) 0.83 [0.91] (H2)	0.64 [0.64]	V(H2,C1)	2.10	1.17 (C1) 0.91 (H2)	0.67
V(H3,C1)	2.02 [2.04]	1.20 [1.13] (C1) 0.81 [0.91] (H3)	0.64 [0.64]	V(H3,C1)	2.10	1.18 (C1) 0.92 (H3)	0.68
V(H4,C2)	2.05	1.21 (C2) 0.83 (H4)	0.64	V(H4,C2)	2.10	1.14 (C2) 0.93 (H4)	0.68
V(H5,C2)	2.01	1.18 (C2) 0.83 (H5)	0.63	V(H5,C2)	2.10	1.19 (C2) 0.93 (H5)	0.69
V(H6,C2)	2.02	1.20 (C2) 0.80 (H6)	0.65				
V(Cl)	2.41 [2.15, 2.15][c]	2.41 [2.15, 2.15] (*Cl*)	1.14 [1.08,1.08]	V(Cl)	2.61	2.57 (*Cl*)	1.20
V(Cl)	2.48 [2.15][c]	2.48 [2.15] (*Cl*)	1.15 [1.08]	V(Cl)	2.61	2.64 (*Cl*)	1.22
V(C1,Cl)	1.35 [1.26]	0.35 [0.53] (C1) 1.00 [0.73] (*Cl*)	0.86 [0.83]	V(Cl)	0.51	0.51 (*C1*)	0.42
V(C2,Cl)	1.35	0.35 (C2) 0.99 (*Cl*)	0.86	V(Cl,C2)	1.46	0.29 (C2) 1.17 (*Cl*)	0.94
				V(C2)	1.54	1.51 (C2)	0.86
				V(C1)	0.51	0.51 (C1)	0.42

[a] All quantities are in electrons. [b] The values in square brackets are for the $ClCH_3$ molecule. [c] There are three monosynaptic V(Cl) basins in $ClCH_3$.

due to the fact that the 6-311++(d,p) basis set is not available for this atom. The same level of theory was used to obtain the wave functions of all the optimized structures. Frequency calculations were performed with the aim to asses the nature of the stationary points. The zero-point vibrational energy corrections were included in all the reported relative energies. All calculations were carried out with the Gaussian 2003 package.[27] The TopMod package[28] was used to analyze the topology of the ELF function. Visual rendering of synaptic basins was carried out with Molekel package[29] using the cube files obtained from TopMod program. The analysis of the charge electron density was performed using the PROAIM package.[30]

4. Results and Discussion

4.1. Geometric and Energetic Analysis. The optimized geometries of all the studied species in the singlet ground-spin state are shown in Figures 1−4. A comparison of the geometrical parameters of the $XC_2H_6^+$ and XC_2H_5 structures reveals the following trend along the series. The CXC angle in the dimethylhalonium cations decreases from 122.4° in $FC_2H_6^+$ to 98.1° in $IC_2H_6^+$, whereas the X−C distance increases from 1.544 Å in $FC_2H_6^+$ to 2.188 Å in $IC_2H_6^+$. In the dimethylhalonium ylides, the value of the CXC angle is nearly constant, between 122 and 123°, whereas the X−CH_2 (X−CH_3) bond distances are around 0.1 Å shorter (longer) than the X−C distance of the corresponding dimethylhalonium cations. We note that this trend is valid only for X = Cl to I, whereas in FC_2H_5 the F−CH_2 bond length is longer than the F−CH_3 distance. In the same figures we have reported the halogen−carbon distance for the XCH_3 molecules (values in square brackets). In all cases the X−C distance in the dimethyl cation is longer than the corresponding distance in the XCH_3 molecule. The

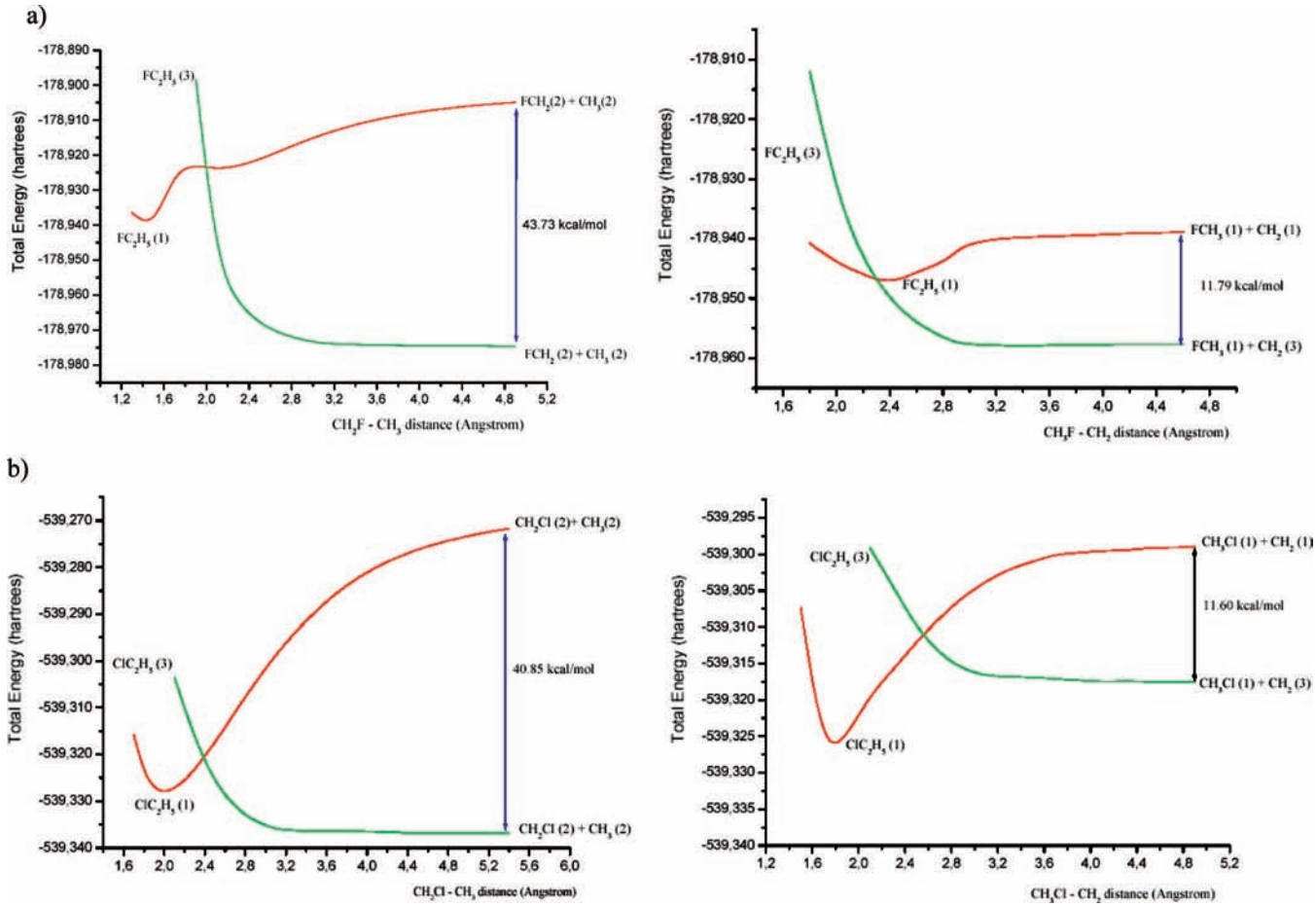

Figure 5. Potential energy profiles of (a) CH_2F-CH_3 (left) and CH_3F-CH_2 (right) and (b) CH_2Cl-CH_3 (left) and CH_3Cl-CH_2 (right). Energies are in hartrees and distances in Å. Spin multiplicities are given in parentheses.

amount of the elongation decreases along the series from 0.149 Å in $FC_2H_6^+$ to 0.015 Å in $IC_2H_6^+$.

The results of the ELF analysis obtained for the initial members of the XC_2H_5 series of structures (section 4.3) have induced us to perform a detailed study of the energetic stability of these structures with respect to the dissociation into fragments ($XCH_2 + CH_3$ and $XCH_2 + CH_3$), taking into account both singlet and triplet spin states. All the triplet spin structures dissociate into two fragments during the optimization process. In the case of the triplet FC_2H_5, the final structure is a hydrogen bond complex, [CH_3F---HCH], with a relative energy (RE) of −0.4 kcal/mol with respect to the $FCH_3 + CH_2$ ground-state fragments. The rest of the XC_2H_5 triplet spin structures have also spontaneously dissociated during the optimization process into $XCH_2 + CH_3$. We must mention that the final dissociated fragments obtained during the optimization ($XCH_2 + CH_3$ or $XCH_2 + CH_3$) are very dependent on the initial geometry, namely, for some initial geometries the final fragments were $XCH_3 + CH_2$ whereas other geometries lead to $XCH_2 + CH_3$. At the present level of theory, the XCH_2 (doublet)[31] + CH_3($^2A_1$) asymptote is more stable than the XCH_3 (^1A) + CH_2 ($^3B_1$) by around 13 kcal/mol, for all the members of the series.

We have analyzed the energetic stability of the optimized XC_2H_5 (X = F, Cl, Br, I) singlet spin structures, with respect to the dissociation into both possible ground-state fragments. The stability of the XC_2H_5 structures with respect to the XCH_2 (doublet)[31] + CH_3 ($^2A_1$) fragments increases in going from F to I, as shown by the corresponding RE values: +22.7, +10.9, +4.8 and −1.2 kcal/mol, respectively.[32] The same trend was found in the case of the dissociation into XCH_3 (^1A) + CH_2 ($^3B_1$), with RE values: +9.9, −2.6, −7.9 and −13.5 kcal/mol, respectively. That indicates, therefore, that the first member of the series, FC_2H_5, is thermodynamically unstable with respect to the dissociation into both considered fragments, whereas ClC_2H_5 and BrC_2H_5 are only unstable with respect to the dissociation into XCH_2 (doublet)[31] + CH_3 ($^2A_1$). The last member of the series is thermodynamically stable with respect to both dissociation processes. To have a better understanding of the bond-breaking processes, we have explored the profiles of the singlet and triplet potential energy curves of all the members of the XC_2H_5 series, along the CH_2X-CH_3 and CH_3X-CH_2 reaction coordinates. The results are collected in Figures 5 and 6. In Figure 5 we report the profiles corresponding to the XC_2H_5 (X = F and Cl, respectively) dissociation into $XCH_2 + CH_3$ (left side) and $XCH_3 + CH_2$ (right side), whereas those of BrC_2H_5 and IC_2H_5 are shown in Figure 6. In that curves, each step corresponds to a partial optimized structure in which the corresponding X−C distance is fixed, whereas all other variables are fully optimized. It can be seen that the triplet spin curves are purely repulsive and that in all cases the dissociation processes from the singlet ground-state XC_2H_5 structures, take place through a crossing between the singlet and triplet potential energy surfaces. That crossing involves in all cases a small barrier height, with the only exception of the dissociation of FC_2H_5 into FCH_3 and CH_2. As will be shown in section 4.3, FC_2H_5 is really formed from two fragments, CH_3F and CH_2. The energy gap of the ground- and excited-state $XCH_3 + CH_2$ dissociated fragments is in all cases around 11.6 kcal/mol

TABLE 4: Basin Populations ($\bar{N}$), Atomic Contributions to Each Basin, and Variance of the Basins, $\sigma^2(\bar{N})$ for Dimethylbromonium and Dimethylbromonium Ylide[a,b]

dimethylbromonium				dimethylbromonium ylide			
basin	$\bar{N}$	atomic contribution	σ^2	basin	$\bar{N}$	atomic contribution	σ^2
C(C1)	2.09 [2.09]	2.09 [2.09] (C1)	0.26 [0.26]	C(C1)	2.09	2.09 (C1)	0.25
C(Br)	27.76 [27.74]	27.76 [27.74] (Br)	1.23 [1.23]	C(Br)	27.76	27.76 (Br)	1.23
C(C2)	2.09	2.09 (C2)	0.26	C(C2)	2.09	2.09 (C2)	0.26
V(H1,C1)	2.02 [2.04]	1.18 [1.13] (C1) 0.84 [0.91] (H1)	0.64 [0.65]	V(H1,C1)	2.06	1.14 (C1) 0.92(H1)	0.68
V(H2,C1)	2.08 [2.05]	1.24 [1.14] (C1) 0.84 [0.91] (H2)	0.65 [0.65]	V(H2,C1)	2.11	1.19 (C1) 0.92 (H2)	0.69
V(H3,C1)	2.04 [2.04]	1.21 [1.13] (C1) 0.82 [0.91] (H3)	0.65 [0.65]	V(H3,C1)	2.08	1.16 (C1) 0.92 (H3)	0.68
V(H4,C2)	2.06	1.22 (C2) 0.84 (H4)	0.65	V(H4,C2)	2.09	1.15 (C2) 0.93 (H4)	0.67
V(H5,C2)	2.04	1.20 (C2) 0.84 (H5)	0.64	V(H5,C2)	2.06	1.13 (C2) 0.93 (H5)	0.68
V(H6,C2)	2.04	1.21 (C2) 0.82 (H6)	0.65				
V(Br)	2.62 [2.25, 2.25][c]	2.62 [2.25, 2.25] (Br)	1.34 [1.22]	V(Br)	2.73	2.73 (Br)	1.41
V(C1,Br)	1.23 [1.25]	0.41 [0.62] (Cl) 0.82 [0.63](Br)	0.83 [0.84]	V(C1,Br)	1.09	0.62 (C1) 0.47 (Br)	0.77
V(Br)	2.69 [2.25][c]	2.68 [2.25] (Br)	1.36 [1.22]	V(Br)	2.79	2.79 (Br)	1.41
V(C2,Br)	1.23	0.81 (Br) 0.42 (C2)	0.83	V(Br,C2)	1.78	0.12 (Br) 1.65(C2)	0.96
				V(Br,C2)	1.24	0.94 (Br) 0.29 (C2)	0.87

[a] All quantities are in electrons. [b] The values in square brackets are for the $BrCH_3$ molecule. [c] There are three monosynaptic V(Br) basins in $BrCH_3$.

TABLE 5: Basin Populations ($\bar{N}$), Atomic Contributions to Each Basin, and Variance of the Basins, $\sigma^2(\bar{N})$ for Dimethyliodonium and Dimethyliodonium Ylide[a,b]

dimethyliodonium				dimethyliodonium ylide			
basin	$\bar{N}$	atomic contribution	σ^2	basin	$\bar{N}$	atomic contribution	σ^2
C(C1)	2.09 [2.09]	2.09 (C1)	0.26	C(C1)	2.09	2.09 (C1)	0.26
C(I)	45.48 [45.49]	45.48 (I)	1.66 [1.66]	C(I)	45.50	45.50 (I)	1.65
C(C2)	2.09	2.09 (C2)	0.26	C(C2)	2.08	2.08 (C2)	0.25
V(H1,C1)	2.04 [2.04]	1.17 (C1) 0.86 (H1)	0.65 [0.66]	V(H1,C1)	2.06	1.12 (C1) 0.94 (H1)	0.67
V(H2,C1)	2.07 [2.05]	1.20 (C1) 0.86 (H2)	0.66 [0.66]	V(H2,C1)	2.09	1.15 (C1) 0.94 (H2)	0.68
V(H3,C1)	2.05 [2.04]	1.19 (C1) 0.86 (H3)	0.66 [0.66]	V(H3,C1)	2.06	1.12 (C1) 0.95 (H3)	0.68
V(H4,C2)	2.06	1.20 (C2) 0.86 (H4)	0.66	V(H4,C2)	2.08	1.13 (C2) 0.95 (H4)	0.68
V(H5,C2)	2.04	1.18 (C2) 0.86 (H5)	0.65	V(H5,C2)	2.05	1.09 (C2) 0.96 (H5)	0.69
V(H6,C2)	2.04	1.18 (C2) 0.86 (H6)	0.66				
V(I)	2.80 [2.36, 2.37][c]	2.79 [2.36, 2.37] (I)	1.47 [1.31, 1.31]	V(I)	2.92	2.91 (I)	1.54
V(C1,I)	1.18 [1.24][c]	0.56 [0.47] (Cl) 0.62 [0.78] (I)	0.81	V(C1,I)	1.14	0.76 (C1) 0.38 (I)	0.79
V(I)	2.84 [2.28]	2.83 [2.28] (I)	1.50 [1.28, 1.28]	V(I)	2.87	2.86 (I)	1.52
V(C2,I)	1.19	0.62 (I) 0.57 (C2)	0.82	V(I,C2)	3.00	0.88 (I) 2.12 (C2)	1.54

[a] All quantities are in electrons. [b] The values in square brackets are for the ICH_3 molecule. [c] There are three monosynaptic V(I) basins in ICH_3.

(Figures 5 and 6). This value agrees well with the singlet−triplet bare CH_2 energy gap (9.215 kcal/mol).[33] For the $XCH_2 + CH_3$ dissociation, the energy gap between the ground and excited-state fragments obtained from the dissociation curves is around 40 kcal/mol, in all cases. That gap should correspond to the transition of one of the fragments to an excited doublet spin state. The lowest-energy doublet excited states of FCH_2 and $ClCH_2$ are very close to that of CH_3, with values that range between 112 and 132 kcal/mol.[34] Therefore, all possible excited dissociated fragments appears to be quite higher in energy than the 40 kcal/mol obtained from the potential energy curves, at the present level of theory. In view of this result, we have also considered the possibility that the singlet spin XC_2H_5 species could disociate into charged species, namely, $XCH_2^- + CH_3^+$ and $XCH_2^+ + CH_3^-$, even when it is a well-known fact that homolytic cleavage is always strongly prefered in the gas phase. In fact, the calculated energy gaps between the charged fragments and the neutral ground-state doublet spin fragments, is much higher (between 200 and 220 kcal/mol). We have not deepened the analysis of the excited-state fragments, which is beyond the scope of this article, but it is possible that the present level of theory is not able to provide a good estimation of the excited-state asymptotes for the singlet spin CH_2X-CH_3 dissociation.

4.2. AIM Analysis. There is a CP of rank (3,−1) in the internuclear area of the halogen and carbon atoms in all of the compounds studied here. In Table 1 are listed the calculated values of the critical point parameters that characterize the C−X bonds. As mentioned in the Computational Details, the basis set employed for iodine (6-311G(d)) is different from that used for the rest of the atoms (6-311++G(d,p)). To check the sensibility of AIM results to the different basis set employed for the last member of the series, for bromine compounds we have performed AIM calculations with both basis sets. It was found that both basis sets yield similar results (Table 1). We consider, therefore, that we can safely analyze the trend of AIM results along the series, even when we have used a slightly different basis set for iodine atom.

All C−X BCP in dimethylhalonium ions (X = Cl, Br, I) display a significant concentration of electronic charge with ρ_b ranging from 0.1089 to 0.1501 au and negative values of $\nabla^2\rho_b$, as in shared type bonds. The energy density E_b at the BCP is

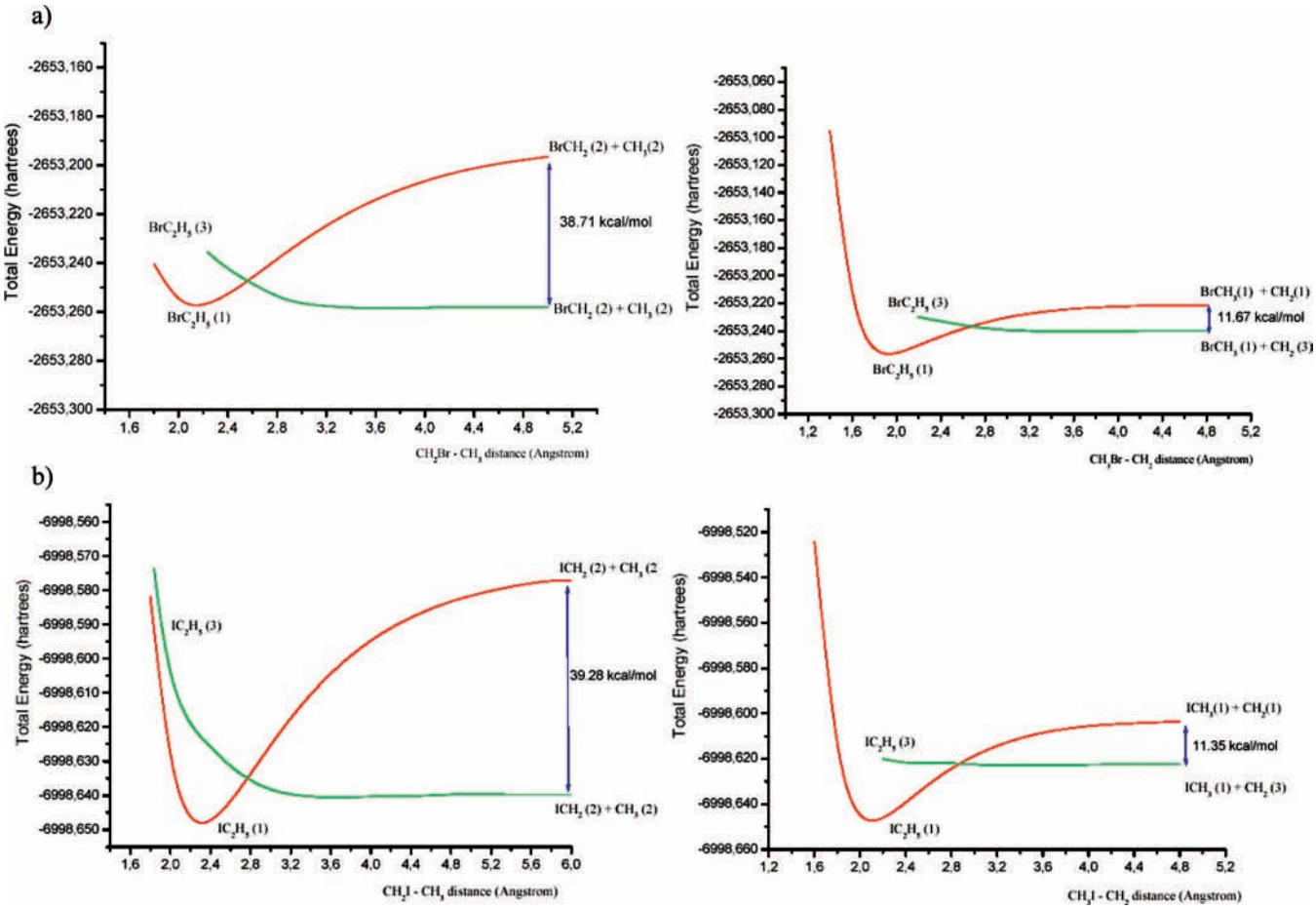

Figure 6. Potential energy profiles of (a) CH_2Br-CH_3 (left) and CH_3Br-CH_2 (right) and (b) CH_2I-CH_3 (left) and CH_3I-CH_2 (right). Energies are in hartrees and distances in Å. Spin multiplicities are given in parentheses.

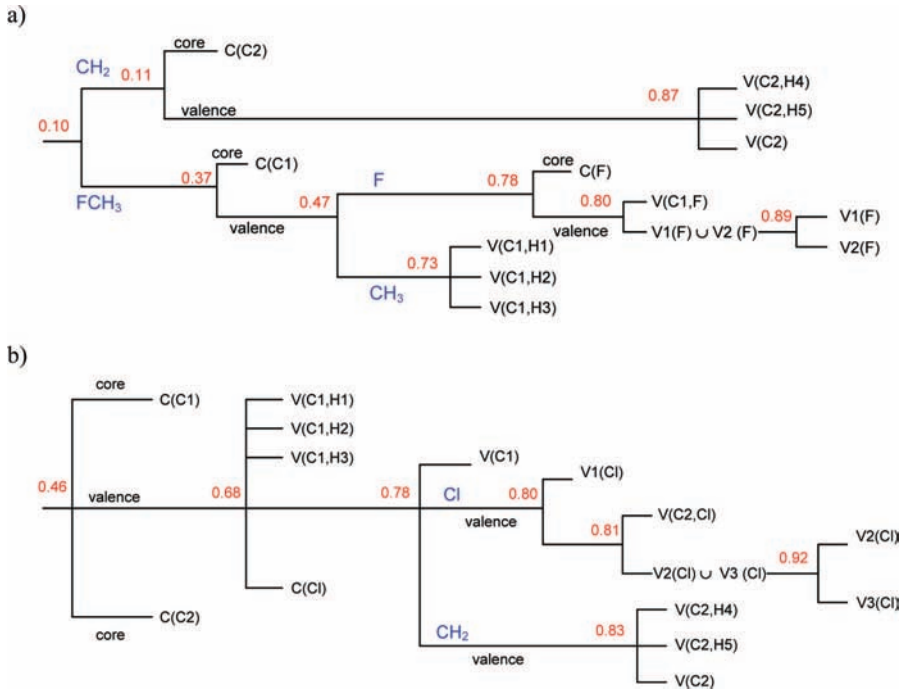

Figure 7. Localization domain reduction tree diagram of (a) FC_2H_5 (^1A) and (b) ClC_2H_5 (^1A).

negative in all cases, which is a typical feature of covalent bonds. The small ellipticity values reveal the cylindrical symmetry of these bonds. The picture of the C−F bonds is particularly interesting. The values of the electron density at the BCP are significant and the ellipticity suggests a local axial symmetry. It seems that this data could point to a single covalent bond; however, the values of $\nabla^2\rho_b$ at the BCP are relatively small and positive. It is necessary to point out that there are cases in

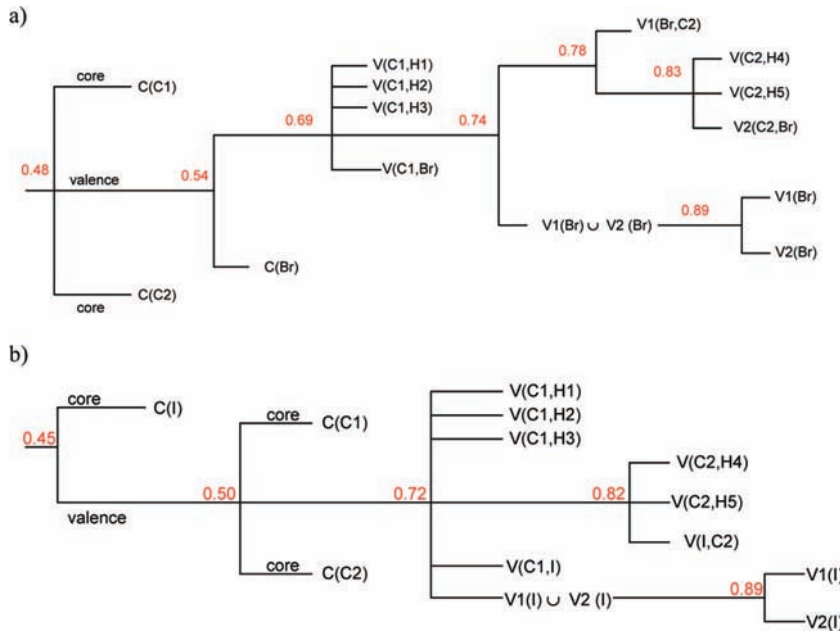

Figure 8. Localization domain reduction tree diagram of (a) BrC_2H_5 (^1A) and (b) IC_2H_5 (^1A).

which the positive value of $\nabla^2\rho_b$ is accompanied by a considerable electronic charge density concentration in the region between the atoms, but this effect is mostly the result of an important charge shifting that is followed by an interatomic surface shifting.[19] In consequence, the BCP would be localized in the positive value region of $\nabla^2\rho_b$. The energy density E_b at the C−F BCP is negative just like happens for covalent bonds. In conclusion, this bond can be considered as an interaction intermediate between closed-shell and shared and be described as a polar bond. Similar results have been previously reported for other molecules containing the C−F bond.[35]

The C−X bond critical points in dimethylhalonium ylides display a behavior typical of shared interactions. Comparing the results obtained for the dimethylhalonium ylides with that of dimethylhalonium ions, we note a decrease of the charge density at the X−CH_3 BCP and an increase of the charge density values at the X−CH_2 BCP, for all the members of the series, with the only exception of FC_2H_5. As mentioned in the previous section, the dimethylfluoronium ylide is the only case in which the F−CH_2 distance is longer than the F−CH_3 bond length. As a consequence of this feature, the charge density has a considerable value at the F−CH_3 BCP and a notably lower value at the BCP linking the CH_2 and the F atom. For the sake of comparison, we have performed the AIM analysis also for the XCH_3 series of compounds. We note that in all cases the charge density at the X−CH_3 BCP is sligthly higher than the corresponding value for the dimethylhalonium cation, which indicates a slight weakening of the X−C bond in going from XCH_3 to $XC_2H_6^+$. The difference, however, decreases notably along the series (see Table 1).

In the Supporting Information (Table S1) we have included the AIM atomic basin populations together with the corresponding variances, $\sigma^2[\bar{N}(\Omega_A)]$, and the atomic charges, for the XCH_3, $XC_2H_6^+$ and XC_2H_5 series. As well, we report the delocalization index, δ(C,X), for the same series of compounds (Supporting Information, Table S2). It can be seen that the delocalization index increases along the XCH_3 series from 0.86 in FCH_3 to 1.14 in ICH_3. We observe, therefore, an increasing of that index with a decreasing in the electronegativity difference between the atoms, in agreement with the trend reported in previous studies concerning this index.[20] The trend is the same for the $XC_2H_6^+$ compounds, with values that are always slightly lower than the corresponding values for the XCH_3 compounds. This can be understood considering that in this series the halogen electrons are delocalized over two carbon atoms. The δ(C,X) indexes corresponding to the X−CH_3 bond in the XC_2H_5 series are systematically lower than the corresponding value for the XCH_3 and $XC_2H_6^+$ homologues, with the only exception being FC_2H_5, which has a value slightly higher than FCH_3. For the X−CH_2 bond of the ylides series there is an increase from the very low value of FC_2H_5 (0.26) to the 1.38 of IC_2H_5. The extremely low value calculated for FC_2H_5 agrees with the description of that moiety obtained from ELF analysis (see next section). The values for the rest of the series range from 1.28 to 1.38, namely between the formal values of bond order 1 and 2, underlying the necessity to invoke different mesomeric structures to explain the CH_3X−CH_2 bonding.

4.3. ELF Analysis. The topological analysis of the ELF function of dimethylfluoronium cation gives rise to ten valence basins, six of which are protonated disynaptic V(C,H) basins, which represent the C−H covalent bonds. The electron population of the V(C,F) basins is very low, namely, 0.81 electrons. Moreover, the standard deviation of that basin population is on the order of $\bar{N}$, and an analysis of the cross-contributions indicates a strong electron delocalization with the fluorine lone pairs. Around 90% of the V(C,F) basin population comes from the F atom. The other two valence basins present in this structure are monosynaptic V(F) basins, which represent the lone pairs of the F atom and have electron populations close to 3 electrons. With the aim of comparison we have performed the ELF analysis also for the XCH_3 series, and we have found that the characteristics of the X−C bonds are very close to that of the cationic series. In the case of FCH_3, the basin population of the V(C,F) basin is slightly higher than that of FC_2H_6 (0.92 e), mainly as a consequence of a greater contribution coming from the C atom. FCH_3 presents three monosynaptic V(F) basins with an electron population of 2.26, 2.24, and 2.12 e, respectively.

The description of the C−F bond provided by the ELF analysis, indicates that they are not classical covalent bonds in which two spin-paired electrons provide the bonding. This type of bonding situation has been often found in atoms bearing lone pairs. The bonding populations are usually significantly lower

than the expected value (in this case 2 electrons), at the expense of increased lone-pair populations. The origin of the so-called lone-pair bond weaking effect (LPBWE) has been extensively studied and its importance has been demonstrated for all atoms.[36] This subject has been analyzed in the context of charge-shift bonding, and it has been found that in ELF analysis it is manifested by a depleted basin population with a large variance and a negative covariance.[36]

Table 2 collects the dimethylfluoronium and dimethylfluoronium ylide basin populations ($\bar{N}$) together with the corresponding variances (σ^2), whereas Figure 1 displays the relevant geometrical parameters and the localization domains of the same molecules. We present for these species the localization domains at two different values of the ELF function, $\eta = 0.85$ and 0.75. The values in square brackets (Table 2 and Figure 1) correspond to FCH_3.

Comparing the results obtained for dimethylfluoronium ylide with that of dimethylfluoronium, we note that as a consequence of the cation deprotonation, the lacking V(C2,H) valence basin is substituted by a monosynaptic V(C2) valence basin with a population of 2.12 electrons. That basin is spatially located in the place of the missing disynaptic basin (Figure 1), offering a strong justification of the molecular geometry and showing a clear agreement with the VSEPR rules. Moreover, this structure is characterized by the absence of a disynaptic V(C2,F) valence basin, which indicates that there is not a covalent bond between the two moieties (FCH_3 and CH_2). We can consider the initial member of the series as an extreme case in which the LPBWE effect is enhanced by the large electronegativity difference and the structure appears as formed by two moieties. As mentioned in the previous sections, the dimethylfluoronium ylide is the only case in the series of ylides studied here, in which the $X-CH_2$ distance is longer than the $X-CH_3$ bond length and is the only singlet-spin-state ylide that is unstable with respect to the dissociation into the $FCH_3(^1A) + CH_2(^3B_1)$ fragments. The electron population of the basins associated to the CH_2 fragment are practically identical to that of the bare singlet-spin-state CH_2. Comparing $FC_2H_6^+$ and FC_2H_5, we note also a slight increase in the V(C1,F) basin population, which is in line with the shortening of the C1−F bond length (Table 2).

In Table 3 are gathered the basin populations for dimethylchloronium, dimethylchloronium ylide and $ClCH_3$. Comparing the results obtained for $ClC_2H_6^+$ with that of $FC_2H_6^+$, we note an increase in the electron population of the disynaptic V(C,Cl) basins (1.35 e), with respect to the 0.81 e of V(C,F), which is accompanied by a simultaneous diminishing of the V(Cl) electron population. The atomic contribution to that basin coming from carbon atom has raised up to 35% of the total population, which can be understood as an increase of the X−C covalent bond character. The rest of the basins are similar to that found in the dimethylfluoronium, namely, six V(C,H) basins with an electron population close to two electrons, and two monosynaptic V(Cl) basins, each one with an electron populations of around 2.5 e.

For dimethylchloronium ylide, we note at first the presence of a disynaptic V(Cl,C2) basin, with a population of 1.46 e, which was missing in the fluoronium homologue. As mentioned in the previous section, in contrast to dimethylfluoronium ylide, the $Cl-CH_2$ distance is notably shorter to the $Cl-CH_3$ one. The increase of the V(Cl) populations with respect to the cation explains the stretching of the CH_3-Cl bond, which becomes *protocovalent*.[37] In fact, at the equilibrium distance the bond between Cl and the CH_3 fragment is characterized by the presence of two monosynaptic valence basins, with an electron population of 0.51 e (Table 3). Within the framework of ELF analysis a covalent interaction is characterized by the splitting of a disynaptic basin into two monosynaptic ones upon bond stretching. In the case of the so-called *protocovalent* bonds that topological change occurs at a bond distance that is shorter than the equilibrium bond length, and that is exactly what happens with the $Cl-CH_3$ bond of chloronium ylide. Therefore, in going from $ClC_2H_6^+$ to ClC_2H_5 we note a reinforcing of the $Cl-CH_2$ bond and a weakening of the $Cl-CH_3$ bond. The rest of the basin are similar to those of FC_2H_5, namely two monosynaptic V(Cl) basins, with electron populations higher than two electrons and a monosynaptic V(C2) basin, with an electron population of 1.54 e that, as in the previous case, is spatially localized in the space of the lacking C−H bond. In Figure 2 are depicted the geometrical structures of dimethylchloronium and dimethylchloronium ylide, as well as the localization domains for isosurfaces of $\eta = 0.83$ and 0.78. For the sake of comparison we have included the calculated Cl-CH_3 bond distancies (values in square brackets).

The topological analysis of the ELF function for dimethylbromonium and dimethyliodonium cations shows the same type of basins of the previously described homologues (Tables 4 and 5, respectively). Comparing the V(C,X) valence populations in the series of the dimethylhalonium ions, we note an initial increase of that population in going from F (0.81 e) to Cl (1.35), followed by a decrease in Br (1.23 e) and I (1.19 e). The higher population of the disynaptic V(C,Cl) basin is accompanied by a corresponding lowering of the V(Cl) basin populations. The same trend is observed in the XCH_3 series.

Comparing the dimethylbromonium and dimethyliodonium ylides with the previous members of the series we note an important increase of the disynaptic V(X,C2) electron populations, which is around 3.0 electrons in both cases. In the case of dimethylbromonium ylide that population is distributed between two different V(C2,Br) disynaptic basins, one of which has a population of 1.78 e and is spatially located in the same position of the V(C2) basin in the previous studied homologues. The contribution to its population coming from Br is around 10% of the total population. The second V(C2,Br) basin has 1.24 e and is located between the center of the C(2) and Br atoms. The Br atom contributes to this basin with around 75% of the total population. The description of the CH_3Br-CH_2 bond obtained from ELF analysis permits to interpret this bond as an hybrid covalent-dative double bond.

In the case of dimethyliodonium ylide, the V(C2,X) basins present in CH_3Br-CH_2 are merged in one V(C2,I) disynaptic basin with a population of 3.0 electrons, which is localized on the C atom. The halogen atom contributes with 30% of the basin population.

The electron population of the V(X,C) basins and the corresponding atomic contributions (Tables 2−5) indicate that the formation of the $XC_2H_6^+$ structures results from the interaction of CH_3X and CH_3^+ and can be interpreted in terms of the superposition of two electrostatically and two dative mesomeric structures[24]

In the case of dimethylhalonium ylides the ELF basin

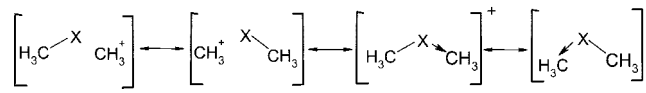

populations and the corresponding covariance matrix of the valence basins show that for BrC_2H_5 and IC_2H_5 the structures can be considered in terms of the resonance structures presented

in Scheme 1. In the case of FC_2H_5 instead the contributing structures are

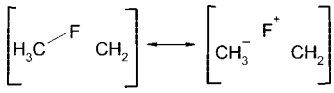

Finally, in the case of ClC_2H_5, ELF analysis indicates that the structure can be interpreted as the superposition of the following resonance structures.

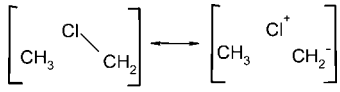

With the aim to complement the population analysis and to clarify the bonding differences between the halonium ylides studied here, we report the localization domain reduction tree diagrams for all the members of the series. These types of diagrams are very useful to discuss the bonding in molecules and complexes and allow us to characterize uniquely the nature of the bonding.[38] Figure 7 displays the reduction diagrams of the singlet ground-state FC_2H_5 and ClC_2H_5 structures, whereas those of BrC_2H_5 and IC_2H_5 are schematized in Figure 8. The bifurcation diagram of FC_2H_5 presents characteristics that distinguish it from the rest of the ylides. Indeed, the first reduction of the FC_2H_5 diagram yields two composite domains corresponding to the interacting moieties (FCH_3 and CH_2), which indicates that such a structure cannot be considered as being chemically bonded. In contrast, the initial parent domain of the rest of the ylides first splits into core domains and a single valence domain that contains all the valence attractors. The fact that the halogen core domains appears at different $\eta(r)$ values is consistent with the different relative electronegativity of the centers. F is the most electronegative atom and therefore preserves its atomic shell structure up to rather high $\eta(r)$ values, whereas iodine is the less electronegative of the series and the core domain splits at the initial bifurcation.

5. Conclusions

In this work, we have used topological methodologies (ELF and AIM analysis) to characterize the X−C (X = F, Cl, Br, and I) bonds in a series of dimethylhalonium ions and dimethylhalonium ylides. The main conclusions brought from this study can be resumed as follows:

1. In AIM analysis, the data describing the bonds of dimethylhalonium ions are typical of covalent bonds. The analyzed $X-CH_3$ bonds are characterized by a relatively large electron density at the BCP and negative values of the energy density. It was shown that the deprotonation of the $XC_2H_6^+$ and the formation of XC_2H_5 results in a decrease of electron density at the BCP of the $X-CH_3$ bond and an increase of the density at the $X-CH_2$ BCP. The exception is dimethylfluoronium ylide in which the topological properties in the $F-CH_3$ bond displays a large contribution of the covalent character, whereas in the $F-CH_2$ bond displays the smallest contribution, a clear indication of a rather weak interaction.

2. ELF analysis shows that in all the studied species (XC_2H_5, $XC_2H_6^+$, XCH_3) the X−C bonds are characterized by depleted basin populations, together with variance values that are of the order of that populations. All V(X,C) basins have strong cross-contributions with their respective V(X) basins, which have in all cases electron populations larger than expected (4 electrons). This type of bonding features has been often found in atoms bearing lone pairs (LPBWE effect), and has been recently analyzed in the context of charge-shift bonding. The description of the bonding provided by ELF indicates that the formation of the $XC_2H_6^+$ structures results from the interaction of CH_3X and CH_3^+ and can be interpreted in terms of the superposition of two electrostatically and two dative mesomeric structures. This interpretation of the bond accounts for the low values of ellipticity at the bcp obtained from AIM analysis and for the low V(C,X) populations.

The formation of the dimethylhalonium ylides can be interpreted considering the deprotonation of the cations, which in a first step substitutes the V(C,H) protonated disynaptic basin by a monosynaptic V(C) that can be involved in a dative bond between the CH_2 and XCH_3 moieties. In the case of FC_2H_5, the large electronegativity difference enhances the LPBWE effect and the deprotonation product appears as formed from two fragments, CH_3F and CH_2. The chloronium ylide is characterized by the presence of a single CH_3X-CH_2 covalent bond, formed mainly from the contribution coming from the halogen atom. In this structure the V(C) monosynaptic basin is still present on the carbon atom. In addition the CH_3-Cl bond has all the characteristics of a *protocovalent* bond. In the case of Br there is a particular type of CH_3Br-CH_2 double bond, which can be considered as an hybrid covalent-dative double bond. For I, the two V(X,C2) basins present in BrC_2H_5 are merged in a disynaptic basin with a population of 3.0 electrons. All the dimethylhalonium ylide structures have been interpreted in terms of two mesomeric structures.

Acknowledgment. Financial support from the Università degli Studi della Calabria is gratefully acknowledged. N.B.O. thanks the Facultad de Agroindustrias and SECYT UNNE for financial support. A.H.J. is a member of the Research Career CIC, Buenos Aires, and N.B.O. is a member of the Research Career of CONICET, Argentina. C.J.A.M. thanks CNPq and FAPERJ for research fellowships.

Supporting Information Available: Table S1 gathers atomic populations and variances, whereas Table S2 shows delocalization indices for all the species studied in this work. This material is available free of charge via the Internet at http://pubs.acs.org.

References and Notes

(1) (a) Olah, G. A. *Halonium Ions*; Wiley: New York, 1975. (b) Olah, G. A.; Laali, K. K.; Wang, Q.; Prakash, G. K. S. *Onium Ions*; Wiley: New York, 1998; Chapter 6.

(2) Roberts, I.; Kimball, G. E. *J. Am. Chem. Soc.* **1937**, *59*, 947.

(3) (a) Olah, G. A.; Bollinger, J. M. *J. Am. Chem. Soc.* **1968**, *90*, 947. (b) Olah, G. A.; Bollinger, J. M.; Brinich, J. M. *J. Am. Chem. Soc.* **1968**, *90*, 2587. (c) Olah, G. A.; Beal, D. A.; Westerman, P. W. *J. Am. Chem. Soc.* **1973**, *95*, 3387.

(4) (a) Olah, G. A.; DeMember, J. R. *J. Am. Chem. Soc.* **1969**, *91*, 2113. (b) Olah, G. A.; DeMember, J. R.; Mo, Y. K.; Svoboda, J. J.; Schilling, P.; Olah, J. A. *J. Am. Chem. Soc.* **1973**, *96*, 884.

(5) (a) Olah, G. A.; DeMember, J. R. *J. Am. Chem. Soc.* **1970**, *92*, 718. (b) Olah, G. A.; DeMember, J. R. *J. Am. Chem. Soc.* **1970**, *92*, 2562. (c) Olah, G. A.; Mo, Y. K. *J. Am. Chem. Soc.* **1974**, *96*, 3560.

(6) (a) Hamilton, T. P.; Schaefer, H. F. *J. Am. Chem. Soc.* **1990**, *112*, 8260. (b) Reynolds, C. H. *J. Chem. Soc., Chem. Commun.* **1990**, 1533. (c) Reynolds, C. H. *J. Am. Chem. Soc.* **1992**, *114*, 8676. (d) Rodriguez, C. F.; Bohme, D. K.; Hopkinson, A. C. *J. Am. Chem. Soc.* **1993**, *115*, 3263. (e) Damrauer, R.; Leavell, M. D.; Hadad, C. M. *J. Org. Chem.* **1998**, *63*, 9476. (f) Teberekidis, V. I.; Sigalas, M. P. *Tetrahedron* **2002**, *58*, 6171.

(7) Olah, G. A.; Rasul, G.; Hachoumy, M.; Burrichter, A.; Prakash, G. K. S. *J. Am. Chem. Soc.* **2000**, *122*, 2737.

(8) (a) Sharma, D. K. S.; Kebarle, P. *J. Am. Chem. Soc.* **1982**, *104*, 19. (b) Jortay, C.; Flammang, R.; Maquestiau, A. *Bull. Soc. Chim. Belg.* **1985**, *94*, 727. (c) Zappey, H. W.; Drewello, T.; Ingemann, S.; Nibbering, N. M. M. *Int. J. Mass Spectrom. Ion Processes* **1992**, *115*, 193. (d) Partanen, T.; Vainiotalo, P. *Rapid Commun. Mass Spectrom.* **1997**, *11*, 881. (e) Freitas, M.; O'Hair, R. A. J. *J. Org. Chem.* **1997**, *62*, 6112.

(9) (a) Beachamp, J. L.; Holtz, D.; Woodgate, S. D.; Patt, S. L. *J. Am. Chem. Soc.* **1972**, *74*, 2798. (b) Bouchoux, G.; Caunan, F.; Leblanc, D.; Nguyen, M. T.; Salpin, J. Y. *Chem. Phys. Chem.* **2001**, *10*, 604.

(10) Glukhovtsev, M. N.; Szulejko, J. E.; McMahon, T. B.; Gauld, J. W.; Scott, A. P.; Smith, B. J.; Pross, A.; Radom, L. *J. Phys. Chem.* **1994**, *98*, 13099.

(11) (a) Murray, D. K.; Chang, J. W.; Haw, J. F. *J. Am. Chem. Soc.* **1993**, *115*, 4732. (b) Jaumain, D.; Su, B. L. *J. Mol. Catal. A: Chem.* **2003**, *197*, 263. (c) Noronha, L. A.; Mota, C. J. A. *Catal. Today* **2005**, *101*, 9.

(12) Haw, J. F.; Song, W. G.; Marcus, D. M.; Nicholas, J. B. *Acc. Chem. Res.* **2003**, *36*, 317.

(13) (a) Olah, G. A.; Doggweiller, H.; Feldberg, J. F. *J. Org. Chem.* **1984**, *49*, 2112. (b) Rimmelin, P.; Taghavi, H.; Sommer, J. *J. Chem. Soc., Chem. Commun.* **1984**, 1210. (c) Chang, C. D.; Hellring, S. D.; Pearson, J. A. *J. Catal.* **1989**, *115*, 282. (d) Blaszkowski, S.; van Santen, R. A. *J. Am. Chem. Soc.* **1997**, *119*, 5020.

(14) Olah, G. A.; Doggwieler, H.; Felberg, J. D.; Frohlich, S.; Grdina, M. J.; Karpeles, R.; Keumi, T.; Inaba, S. I.; Ip, W. M.; Lammertsma, K.; Salem, G.; Tabor, D. C. *J. Am. Chem. Soc.* **1984**, *106*, 2143.

(15) Ando, W.; Kondo, S.; Migata, T. *J. Am. Chem. Soc.* **1969**, *91*, 6516.

(16) Sheppard, W. A.; Webster, O. W. *J. Am. Chem. Soc.* **1973**, *95*, 1695.

(17) (a) Doyle, M. P.; Tamblyn, W. H.; Bagheri, V. *J. Org. Chem.* **1981**, *46*, 5094. (b) Padwa, A.; Hornbuckle, S. F. *Chem. Rev.* **1991**, *91*, 263.

(18) Noronha, L. A.; Judson, T. J. L.; Dias, J. F.; Santos, L. S.; Eberlin, M. N.; Mota, C. J. A. *J. Org. Chem.* **2006**, *71*, 2625.

(19) Bader, R. F. W. *Atoms in Molecules. A Quantum Theory*; University Press: Oxford, 1990.

(20) (a) Fradera, X.; Austen, M. A.; Bader, R. F. W. *J. Phys. Chem. A* **1999**, *103*, 304. (b) Fradera, X.; Poater, J.; Simon, S.; Duran, M.; Solà, M. *Theor. Chem. Acc.* **2002**, *108*, 214. (c) Ángayán, J. G.; Loos, M.; Mayer, I. *J. Phys. Chem.* **1994**, *98*, 5244. (d) Poater, J.; Duran, M.; Solà, M.; Silvi, B. *Chem. Rev.* **2005**, *105*, 3911. (e) Fradera, X.; Solà, M. *J. Comput. Chem.* **2002**, *23*, 1347.

(21) Becke, A. D.; Edgecombe, K. E. *J. Chem. Phys.* **1990**, *92*, 5397.

(22) (a) Silvi, B.; Savin, A. *Nature* **1994**, *371*, 683. (b) Savin, A.; Silvi, S.; Colonna, F. *Can. J. Chem.* **1996**, *74*, 1088.

(23) Savin, A.; Flad, J.; Preuss, H.; von Schnering, H. G. *Angew. Chem.* **1992**, *104*, 185.

(24) (a) Silvi, B. *Phys. Chem. Chem. Phys.* **2004**, *6*, 256. (b) Lepetit, C.; Silvi, B.; Chauvin, R. *J. Phys. Chem. A* **2003**, *107*, 464. (c) Pilme, J.; Silvi, B.; Alikhani, M. E. *J. Phys. Chem. A* **2005**, *109*, 10028.

(25) (a) Becke, A. D. *Phys. Rev. A: At., Mol., Opt. Phys.* **1988**, *38*, 3098. (b) Lee, C.; Yang, W.; Parr, R. G. *Phys. Rev. B: Condens. Matter* **1987**, *38*, 785.

(26) (a) Clark, T.; Chandrasekhar, J.; Spitznagel, G.W.; Schleyer, P. v. R. *J. Comput. Chem.* **1983**, *4*, 294. (b) Curtiss, L. A.; McGrath, M. P.; Blandeau, J.-P.; Davis, N. E.; Binning, R. C., Jr.; Radom, L. *J. Chem. Phys.* **1995**, *103*, 6104. (c) Curtiss, L. A.; McGrath, M. P.; Blandeau, J.-P.; Davis, N. E.; Binning, R. C., Jr.; Radom, L. *J. Chem. Phys.* **1995**, *103*, 6104.

(27) Frisch, M. J.; Trucks, G. W.; Schlegel, H. B.; Scuseria, G. E. M.; Robb, A.; Cheeseman, J. R.; Montgomery, J. A., Jr.; Vreven, T.; Kudin, K. N.; Burant, J. C.; Millam, J. M.; Iyengar, S. S.; Tomasi, J.; Barone, V.; Mennucci, B.; Cossi, M.; Scalmani, G.; Rega, N.; Petersson, G. A.; Nakatsuji, H.; Hada, M.; Ehara, M.; Toyota, K.; Fukuda, R. Hasegawa, J. Ishida, M.; Nakajima, T.; Honda, Y. Kitao, O.; Nakai, H.; Klene, M.; Li, X.; Knox, J. E.; Hratchian, H. P.; Cross, J. B.; Bakken, V.; Adamo, C.; Jaramillo, J.; Gomperts, R.; Stratmann, R. E.; Yazyev, O.; Austin,; A. J.; Cammi, R.; Pomelli, C.; Ochterski, J. W.; Ayala, P. Y.; Morokuma, K.; Voth, G. A.; Salvador, P.; Dannenberg, J. J.; Zakrzewski, V. G.; Dapprich, S.; Daniels, A. D.; Strain, M. C.; Farkas, O.; Malick, D. K.; Rabuck, A. D.; Raghavachari, K. Foresman, J. B.; Ortiz, J. V.; Cui, Q. Baboul, A. G.; Clifford, S. Cioslowski, J.; Stefanov, B. B. Liu, G.; Liashenko, A.; Piskorz, P.; Komaromi, I.; Martin, R. L.; Fox, D. J.; Keith, T.; Al-Laham, M. A.; Peng, C. Y.; Nanayakkara, A.; Challacombe, M. W.; Gill, P. M.; Johnson, B.; Chen, W.; Wong, M. W.; Gonzalez, C.; Pople, J. A. *Gaussian 03*, revision C.02; Gaussian, Inc.: Wallingford, CT, 2003.

(28) Noury, S.; Krokidis, X.; F. Fuster, B. Silvi, *TopMod Package*; Paris, 1997. (b) Noury, S.; Krokidis, X.; Fuster, F.; Silvi, B. *Comput. Chem.* **1999**, *23*, 597.

(29) Flükiger, P. Lüthi, H. P. Portmann, S. Weber, J. *MOLEKEL 4.0*; Swiss Center for Scientific Computing, Manno, Switzerland, 2000.

(30) Biegler-König, F. W.; Bader, R. F. W.; Tang, T. H. *J. Comput. Chem.* **1982**, *13*, 317.

(31) The ground states of FCH_2 and $ClCH_2$ have $^2B_1$ symmetry, whereas $BrCH_2$ and ICH_2 have ^2A.

(32) The relative energy (RE) values are calculated as the energetical difference between the energy of the singlet XC_2H_5 structures and the corresponding fragments, namely, $[E(XC_2H_5) - E(XCH_3) - E(CH_2)]$ and $[E(XC_2H_5) - E(XCH_2) - E(CH_3)]$, respectively. In all cases the species are in their ground state and the energies include the zero-point energy correction.

(33) Jensen, P.; Bunker, P. R. *J. Chem. Phys.* **1988**, *89*, 1327.

(34) Levchenko, S. V.; Krylov, A. I. *J. Chem. Phys.* **2001**, *115*, 7485.

(35) Roohi, H.; Ebrahimi, A. J. *Mol. Struct. (THEOCHEM)* **2005**, *726*, 141.

(36) (a) Shaik, S.; Maitre, P.; Sini, G.; Hiberty, P. C. *J. Am. Chem. Soc.* **1992**, *114*, 7861. (b) Bil, A.; Latajka, Z. *Chem. Phys.* **2004**, *303*, 43. (c) Shaik, S.; Danovich, D.; Silvi, B.; Lauvergnat, D. L.; Hiberty, P. C. *Chem. Eur. J.* **2005**, *11*, 6358, and references therein.

(37) Llusar, R.; Beltrán, A. M.; Andrés, J.; Noury, S.; Silvi, B. *J. Comput. Chem.* **1999**, *20*, 1517.

(38) Silvi, B. *J. Mol. Struct.* **2002**, *614*, 3.

JP805699X